PERGAMON

Journal of Structural Geology 22 (2000) 159–168

JOURNAL OF STRUCTURAL GEOLOGY

www.elsevier.nl/locate/jstrugeo

Growth of a normal fault system: observations from the Lake Malawi basin of the east African rift

Juan Contreras, Mark H. Anders*, Christopher H. Scholz

Department of Earth and Environmental Sciences and Lamont-Doherty Earth Observatory, Columbia University, Palisades, NY 10964, USA

Received 8 July 1998; accepted 22 September 1999

Abstract

We have studied the growth history of the Usisya normal fault system, which bounds the west side of the Lake Malawi basin, one of the largest rift basins in the east African rift system. The Lake Malawi rift basin is a complex of intrabasins and intrabasin highs formed by three major fault segments, each about 100 km in length. The basin has been actively subsiding since the late Miocene, and has a maximum depth of about 3 km. Unlike the majority of previous studies of fault systems, we are able to define the temporal evolution of this fault system using the patterns of sediment infill. This is due almost exclusively to the availability of a high-density seismic reflection network in combination with several clearly identifiable temporal marker beds. An analysis of the seismic reflection data reveals that growth of the basin-bounding faults occurred in the following sequence: 1) In the early stages of rifting (starting about 8.6 Ma), the northern fault was the most active, 2) then, extension shifted to the southernmost fault segment and lasted until about 2.5 Ma, 3) during the interval between about 2.3 Ma and 1.6 Ma, the central segment was most active. Prior to the last interval, the central segment accrued the least total displacement of the three segments. This contradicts the common notion that the location of maximum displacement remains at a fixed location from fault inception or that the largest fault in any population of faults always maintained the highest displacement rate. Consistent with observations on smaller faults, there is a marked increase in the displacement gradient on individual faults in the regions of overlapping segments. Although there is an observable asymmetry in individual segment displacement-profiles, there is a clear evolution toward a flattened 'bell shaped' total displacement profile for the fault system that is consistent with the shape and scaling relationships of displacement vs. length that are observed on a wide range of individual normal faults. This suggests that the irregularities in the shape and scaling relationships observed in complex fault systems will eventually smooth-out. Moreover, the observed growth pattern suggests that the profile of the fault system will progress toward that of isolated faults, provided the system is allowed sufficient time to evolve. This in turn describes a process for maintaining a self-similar scaling observed in large populations of faults, which span several orders of magnitude in fault length.

1. Introduction

How systems of normal faults interact during growth has been the subject of several recent studies (Peacock and Sanderson, 1991; Anders and Schlische, 1994; Trudgill and Cartwright, 1994; Dawers and Anders, 1995; Cartwright et al., 1995; Cartwright and Mansfield, 1998). The process of growth and linkage is enigmatic since the only observable is the final displacement of the individual faults with little or no record of the temporal succession of faulting. Independent of the temporal progression, these studies of final displacement distribution clearly show a relationship between fault displacement patterns on individual fault segments and their proximity to other segments within the fault system. Typically the faults show a marked increase in the displacement gradient at the tips of faults that are overlapping (e.g. Peacock and Sanderson, 1991; Trudgill and Cartwright, 1994; Cartwright and Mansfield, 1998), provided the segments are in close enough proximity to allow their re-

* Corresponding author.
E-mail address: manders@ldeo.columbia.edu (M.H. Anders).

0191-8141/00/$ - see front matter
PII: S0191-8141(99)00157-1

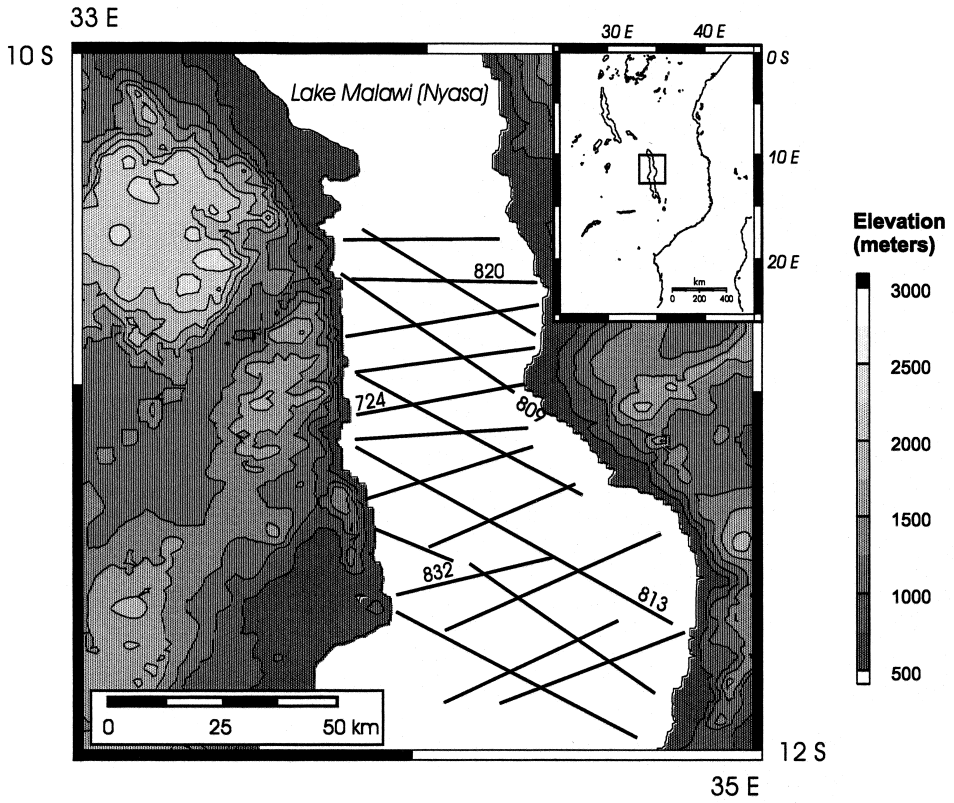

Fig. 1. Location of Lake Malawi (Nyasa) rift in east Africa. This figure also shows the traces of 19 seismic lines collected by the Project PROBE (Scholz, 1989).

spective stress fields to interact during growth. Individual normal faults within a particular tectonic setting have been observed to have displacement vs. length ratios that are scale independent (Dawers et al., 1993). Field observations by Dawers and Anders (1995) and Schlische et al. (1996) have shown that linked fault systems, within a common lithologic and tectonic environment, also scale in a self-similar manner in comparison to isolated individual faults, even though segments within the larger system express asymmetric displacement patterns. Their conclusion was that smaller faults within the region of overlap/linkage sum displacement with the overlapped segments to produce a flattened bell-shaped profile resembling that of individual isolated faults. If true, the linkage process must evolve in a way that allows displacement deficits in the areas of overlap/linkage to be eliminated. It is this temporal evolution that we investigate here.

Structural analysis and high resolution stratigraphy of rift basins have documented the first order time-dependent behavior of large fault systems (10^4–10^5 m) in time scales of 10^6–10^7 y (Rosendahl, 1987; Schlische and Anders, 1996). Seismicity studies, with the help of computer models, have revealed short term fault interactions (10^2 y) due to constructive and destructive interference patterns of the stress fields surrounding faults (King et al., 1994; Hodgkinson et al., 1996; Deng and Sykes, 1997). Quasi-static finite and boundary element methods have further investigated these stress interactions in faults with an en échelon array (Pollard and Segall, 1980; Willemse et al., 1996; Crider and Pollard, 1998). More recently, scalar and spring-block models have started to address the problem of fault nucleation and growth by linkage of segments (Spyropoulos et al., 1997; Gupta et al., 1998).

In this study we document how large normal faults of the Usisya fault system in central Lake Malawi rift grew and interacted during the last 8.6 Ma. In particular we have been able to establish the sequence of faulting for the Usisya fault system and, most importantly, the direction of propagation of individual faults within this system and how their along-strike displacement profiles (displacement distribution) develop through time.

2. Geologic setting

Lake Malawi rift is the southern termination of the east African rift system, and like many other rift basins, is made up of a series of linked half graben

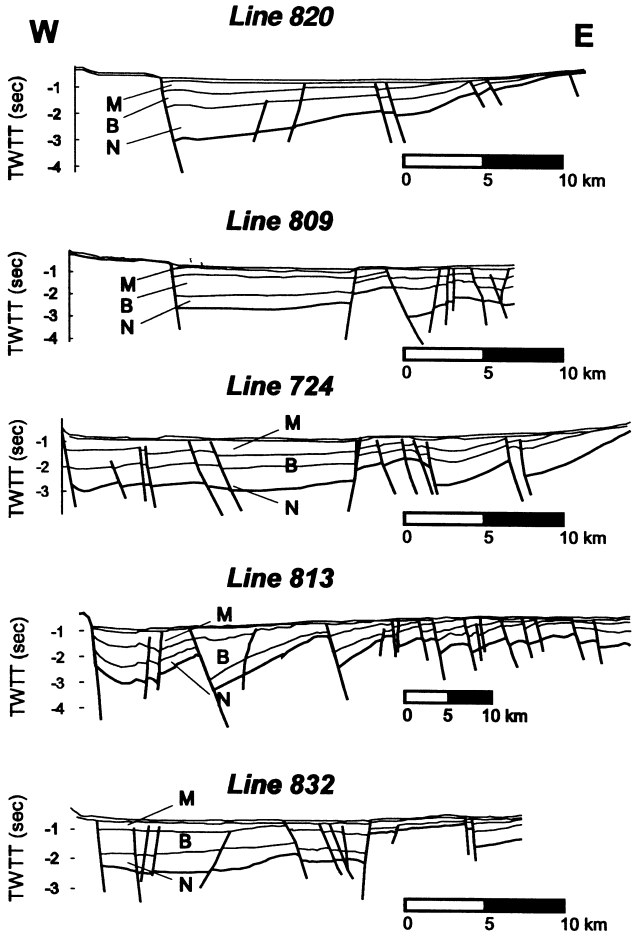

Fig. 2. Examples of four line drawing interpretations of seismic profiles from the Lake Malawi rift (Scholz, 1989). See Figs. 1 and 3 for location of these lines. Like many other rift basins Lake Malawi has a half graben geometry. The seismic stratigraphy consists of four major seismic sequences, Nyasa (N), Boabab (B), Mbamba (M) and Songwe (not shown) bounded by three unconformities Nyasa–Boabab, Boabab–Mbamba, and Mbamba–Songwe (Flannery and Rosendahl, 1990).

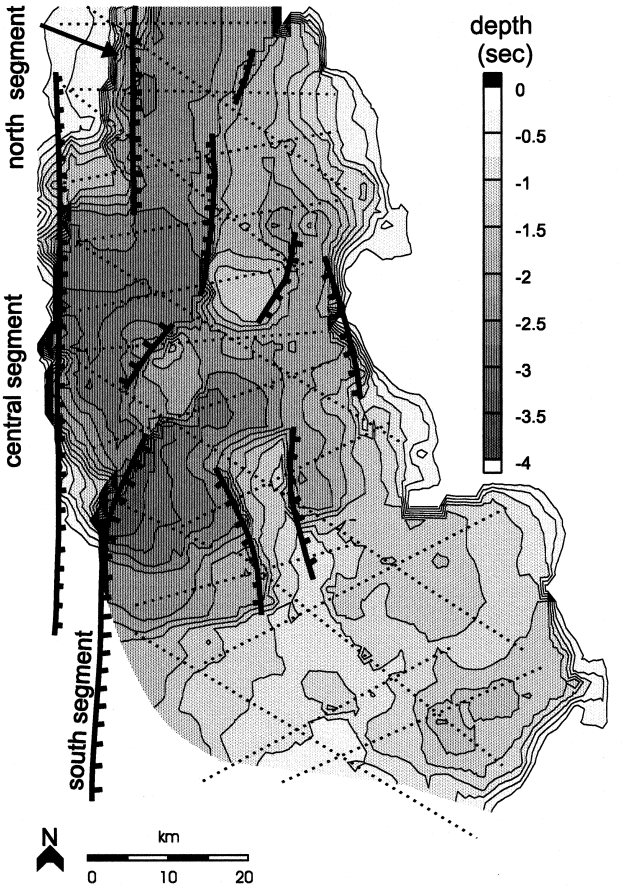

Fig. 3. Simplified structural map of the acoustic basement of the central part of Lake Malawi rift. This interpretation is based on a 1 km × 2 km grid obtained from the lines shown in Fig. 2. Structurally, this part of the basin consists of three steep normal faults (the Usisya fault system), along the western shore of the lake, and by a system of intrabasinal highs sub-parallel to the fault bounding system.

(Fig. 1) bounded on one side by steeply dipping normal faults. The central part of Lake Malawi rift consists of a series of normal faults (border fault system) with a north–south orientation and a series of internal horsts also striking in a north–south direction (Figs. 2 and 3). Scholz (1989) originally described the border fault system as composed of two faults. However, our analysis indicates that it is composed of three major bounding faults each about 100 km long (Fig. 3). For the purposes of this paper we have named the segments of the Usisya fault system the north, central and south segments. These partially overlapping fault segments each have a maximum basin depth of between 3 and 3.5 s two-way-travel-time corresponding roughly to a hanging wall downdrop of about 3 km depth. For the most part the footwall has been removed by erosion and therefore restoration of total displacement requires some estimation. Assuming that the footwall uplift is roughly equivalent to hanging wall downdrop (see Anders et al., 1993), the maximum displacement on this fault is just under 6 km (see Section 3.1 for discussion of velocity structure used). The displacement to length ratio of the combined segments is 0.03, which is consistent in magnitude with measurements of displacement vs. length found on other extensional small fault systems (see Schlische et al., 1996).

Spacing between the three segments is about 10 km and although the seismic data are not sufficient to resolve linkage at depth, a 10-km spacing is great enough to suggest that the major fault segments are not physically linked.

Some uncertainty exists regarding the ages of the seismic sequences we use to assess fault growth in the northern Malawi basin. No drilling data link seismic reflections with basin stratigraphy. Moreover, we use reflections from apparent unconformities, which by their nature represent omission of time, and thus are

difficult to date. A significant effort to correlate the seismic sequences to units exposed at the surface and to rock types based on their seismic reflectance characteristics has been undertaken by Flannery and Rosendahl (1990) and Ebinger et al. (1993). We choose to assign seismic stratigraphic units based on the unconformity nomenclature assigned by Flannery and Rosendahl (1990). The seismic sequences we defined, from bottom to top, are Nyasa, Boabab, Mbamba and Songwe. Assigning ages to these units is difficult because attempts to correlate using isotopic dates from directly north of Lake Malawi (Ebinger et al., 1993) lump the lower two units together and define a reflection within the Mbamba sequence. Nevertheless, it is clear the earliest sequence formed a short time before about 8.6 Ma (Ebinger et al., 1993). At sometime after 6.33 Ma to about 2.5 Ma the next sequence was deposited. As we define the Mbamba sequence, using the dates published in Ebinger et al. (1993), deposition initiated between 2.3 Ma and 2.25 Ma and continued to about 1.6 Ma. The upper most sequence, the Songwe sequence, was continuously deposited from about 1.6 Ma into the latest Pleistocene.

As with the dating of the seismic sequences, the assignment of lithology for these sequences is not based on direct observations. The dominant basal reflection probably comes from the Carboniferous to Permian Karoo rocks, overlain by Mesozoic dinosaur beds. Where exposed at the surface, these units are mudstones, siltstones, arkoses and conglomerates. These units overlie Precambrian mylonites and gneisses for which the seismic boundary is poorly imaged. The lowest sequence, the Nyasa sequence, consists of fluvo-lacustrine sediments interbedded with distal volcanic units. The upper sequences are more representative of open lake environments (Flannery and Rosendahl, 1990). Their seismic reflection character is consistent with muds interbedded with silts and fine sands (see Flannery and Rosendahl, 1990).

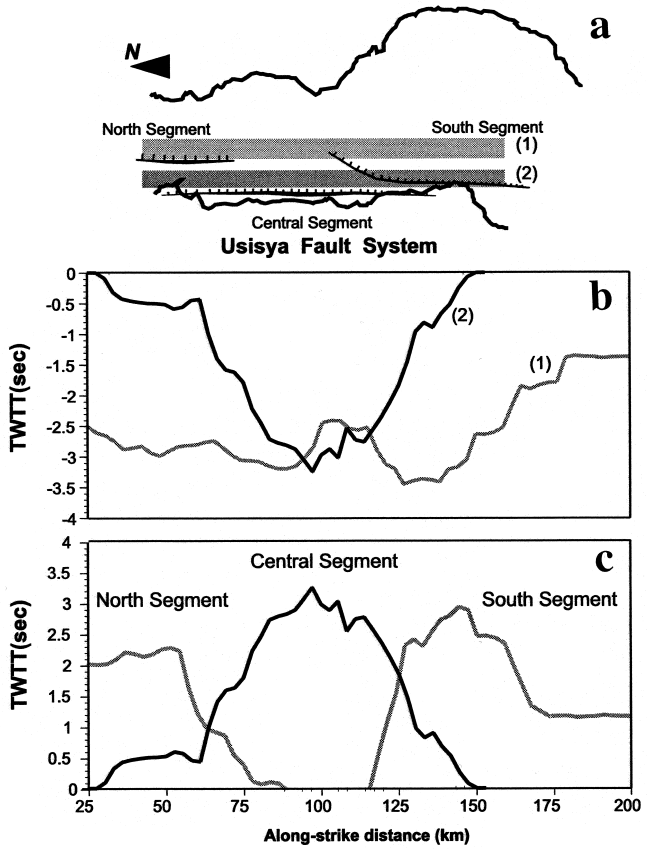

Fig. 4. Methodology employed in estimating the along-strike displacement on each of the faults of the bounding system. Here we used the lake level and the acoustic basement as reference horizons but any of the unconformities can be used as well. First, we averaged the depth of the acoustic basement of the shaded regions in (a); these averaged values are shown in (b). Light gray line in (b) corresponds to shaded area adjacent to the North and South fault segments, solid black line comes from the area adjacent to the central segment and relay ramp zones. The averaged value of the innermost area (solid black line in b) represents the total displacement, in two-way-traveltime (twtt), due to the three fault segments of the bounding system. The averaged depth, in twtt, of the basement over the relay ramp zones (light gray line in b) represents the displacement of the central fault segment. Finally, the displacement of the northern and southern segments can be calculated by taking the difference of these two curves (c). Observe that in this last plot we inverted the values of the vertical axis.

3. Data set and methodology

The data set used to assess the evolution of the Usisya bounding fault system consists of a subset of 19 high-resolution unmigrated seismic lines of the 65 lines (3500 km) originally collected, processed, and interpreted by the PROBE project and published by Scholz (1989). A set of 12 lines have an east–west orientation and are about 8 km apart (Fig. 1). The remaining seven lines have a northeast–southwest orientation; separation between these lines is about 15 km (Figs. 1 and 2). While resolution is practically continuous in an east–west direction, stratigraphic and structural information is discrete in the north–south direction. Therefore, we have carried out an interpolation to reconstruct the geometry of the basement as well as the geometry of the seismic sequences in this basin. Observe that from the separation of the lines only structures with a wavelength of the order of 40 km can be accurately resolved and that the minimum interpolation interval is 2 km in a north–south direction. Fig. 3 shows an interpretation of the structure of the acoustic basement based on our interpolation.

Once the acoustic basement, the Nyasa–Boabab, the Boabab–Mbamba, and the Boabab–Songwe sequence unconformities were interpolated to a regular grid with a unit cell of 2.0 km (north–south) × 1 km (east–west),

the thickness of the Nyasa, Boabab, and Mbamba units could be calculated. We decided not to use the Songwe sequence because its thickness only averages 100 m (0.1 s two-way-travel-time). The distribution of thicknesses of these various units then permits assessment of along-strike displacement profiles for each of the major fault segments. To make these estimations we assumed the following: i) sedimentation adjacent to the bounding system is controlled by faulting; ii) a continuous supply of sediments; iii) the bounding unconformities represent small hiatuses compared with the total history of the basin; iv) the current water surface is the neutral point between footwall uplift and hanging wall downdrop, and that the basin could not have been filled above this level (460 m a.s.l.); and v) at every time interval the basin was completely filled with sediments. Our first assumption is justified by the high relief of the footwall block (1500 m above the lake level). The footwall block constitutes a natural barrier to large rivers forcing them to enter the basin at an axial position or on the hanging wall block. Our second and third assumptions can be justified by the fact that this basin has remained in hydrological equilibrium (water input = water loss) during most of its history (Scholz, 1997). Assumption (iv) is justified by the fact that hanging wall downdrop and footwall uplift are related to the datum of the African craton (see Vening Meinesz, 1950), and that lake outlets should also be fixed to that datum. Even if lake levels rise and fall due to climate variations, as long as the lake's outlet is fixed to the cratonal datum, under-filling of the basin can be accounted for (see source of errors later in text). Clearly our fifth assumption does not hold, as currently Lake Malawi is one of the deepest lakes in the world (about 700 m deep), and there is no reason to think the modern lake is an exceptional stage in the history of the basin. However, we can use this information to estimate error bars in our estimations.

The plot shown in Fig. 4 illustrates how we obtained the displacement profiles for the faults of the Usisya system using the methodology described above. In order to interpret these data three important considerations must first be made. First, by displacement we mean the vertical component of the displacement vector for the hanging wall only. The horizontal components cannot be fully recovered from the seismic stratigraphy alone. Second, displacement or depth is represented in two-way-travel-time (in seconds). A manual migration and a time–depth conversion assuming a linear increase of velocity with travel time, using a velocity gradient of 750 m/s (Flannery and Rosendahl, 1990), have demonstrated that the results presented here are not substantially changed. Conveniently, two-way-travel-times, in seconds, roughly correspond with the converted depths, in kilometers. Third, since we are using the thickness of the seismic units, we are estimating only subsidence associated with the faults.

In many normal faults the ratio of uplift of the footwall block vs. subsidence of the hanging wall is close to 1:1, when footwall erosion is taken into account. Lower footwall uplift ratios are commonly reported in the literature for developed normal fault basins. However, almost all such basins are associated with footwalls exhibiting significant loss due to erosion. Studies that account for an eroded footwall exhibit ratios verging on 1:1, though always slightly less than 1:1 (see Anders et al., 1993, for further discussion). Therefore, our assessment of total displacement for the Usisya fault system should be about twice the downthrow shown in Fig. 4. In Fig. 4, and in the subsequent plots, we have included the total displacement curve, which is the sum of the hanging wall displacement of individual faults projected in the assumed extension direction (oriented at a right angle to the fault systems' strike). The shape of this curve has commonly been used as a parameter-signalling interaction of fault segments (Dawers and Anders, 1995; Willemse, 1997; Peacock and Sanderson, 1994). This will be discussed in detail in Section 5.

3.1. Sources of error

There are several sources of error possible involved in relating two-way-travel-time from seismic reflection lines to displacement. These include compaction of sediments, accurate location of reflections, water depth during the interval over which sediments are accumulated, estimating the elevation of a point from which downdrop displacement can be measured, and in the case of assessing total displacement, estimating the maximum offset position on the eroded footwall.

We deal with the problem of compaction by adjusting the velocity as a function of the age/depth of each unit based on our experience in working with velocity logs from boreholes in other normal fault basins. Our estimate is 3.0 km/s for the older Nyasa sequence, 2.0 km/s for the Boabab sequence, and 1.8 km/s for the Mbamba sequence, the youngest sequence. Further data, say from drilling in the basin, could be used to recalculate our measurement at a later time, although we suspect the values we have chosen will not make a significant difference to our results. Moreover, these kinds of assumptions about the velocity structure are routinely made in seismic stratigraphy studies.

The error in measuring the two-way-travel-time of any given reflection is so small that it is incorporated in the thickness of the symbol used. However, the problem of estimating downthrow not associated with concomitant sediment infill is more difficult to constrain. This is a problem that relates to the fact that

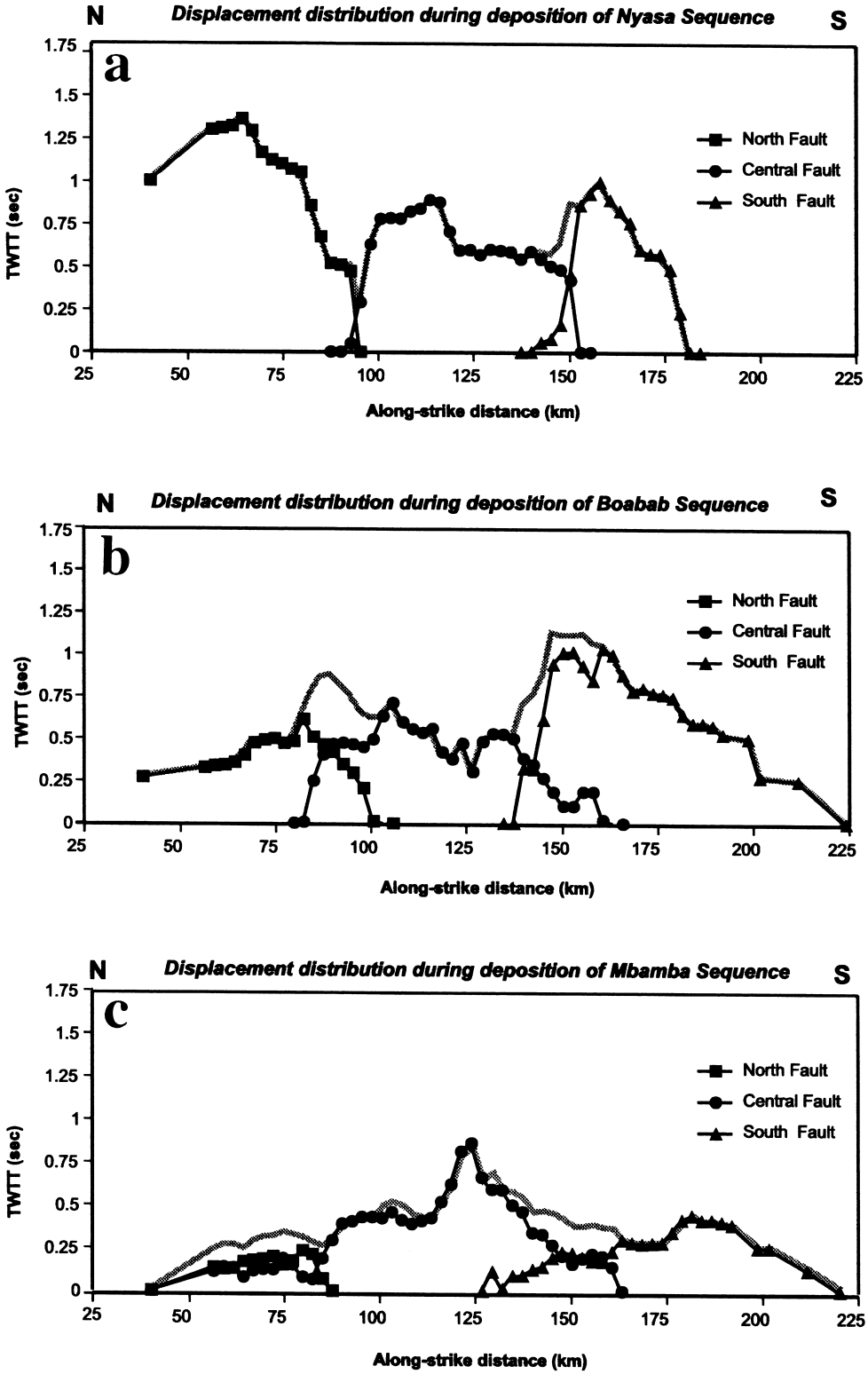

Fig. 5. (a) Along-strike displacement profiles of the three faults of the Usisya fault system as inferred from the thickness distribution of the Nyasa sequence. Light gray line is the sum of the displacement of these three faults. The vertical scale is two-way-travel-time in seconds. (b) Along-strike displacement profiles for the three faults of the Usisya fault system as inferred from the thickness distribution of the Boabab sequence. Light gray line is the sum of the displacement of these three faults. The vertical scale is two-way-travel-time in seconds. (c) Along-strike displacement profiles of the three faults of the Usisya fault system as inferred from thickness distribution of the Mbamba sequence. Light gray line is the sum of the displacement of these three faults. The vertical scale is two-way-travel-time in seconds.

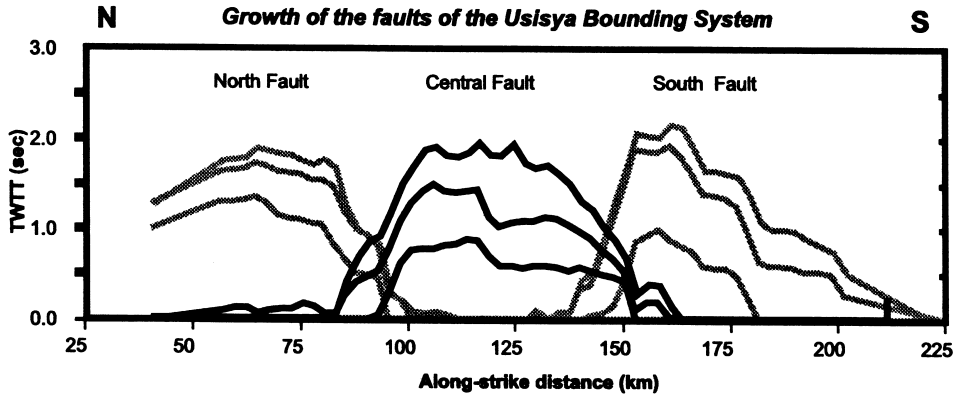

Fig. 6. Cumulative plot showing how the three segments of the Usisya system increased their length and displacement. Each line corresponds to the summed displacement accommodated during the deposition the previous sequences. Vertical scale is two-way-travel-time in seconds.

Lake Malawi exists. In other words, the presence of a maximum of 700 m of water above the basin sediment fill suggests the basin is growing faster than sediment can fill the created void. Therefore, a current measurement of total downthrow based on sediment thickness will underestimate displacement by as much as 700 m. What is more, this could have been the case at any time during the deposition of the sedimentary sequences filling the basin. Consequently, in our displacement profiles (Fig. 5a), we may have excluded an additional 700 m of displacement by considering the thickness of the sequences alone and by ignoring the presence of the lake. However, we have included 700 m of downthrow in our calculation for determining the displacement to length ratio for all faults considered.

To get total displacement we must assume that the hanging wall downdrop has some proportionality to the footwall uplift. Here, we assume, as discussed before, a ratio of 1:1. This determination also assumes that the present lake level represents the mid-point/line datum of displacement. This is a hidden assumption built into almost all estimates of displacement on normal faults where the hanging wall sediments are the sole measure of offset.

4. Results

The displacement distribution of the three faults of the Usisya fault system during the deposition of the Nyasa sequence (starting about 8.6 Ma) is shown in Fig. 5(a). As seen in this figure, the north fault segment was the most active during early rifting. The other two fault segments were also active, but exhibit a lower total displacement over the same interval. During the next interval (ending just after 2.5 Ma) while the Boabab sequence was deposited, the southern segment was almost twice as active as the other main segments of the fault (Fig. 5b). During the last interval (between about 2.3 Ma and 1.6 Ma when the Mbamba sequence deposited), the central segment was almost twice as active as the northern and southern segments (Fig. 5c).

The results presented above agree with the stratigraphic analysis of Lake Malawi rift by Flannery and Rosendahl (1990). Both studies are based on the assumption that sediment thickness is solely controlled by the activity of the faults. Though other interpretations that could account for differential thicknesses are equally plausible, for example, the build-up of relief by sedimentary processes, several pieces of evidence support this assumption. i) The internal geometry of the reflectors of the oblique lines (Fig. 1) is basically sub-parallel and thickens toward the bounding fault system. The only place where reflectors reveal clinoforms, possibly associated with deltas, is the north relay ramp area, having a thickness of 300 m (Flannery and Rosendahl, 1990). ii) Even if one considers processes such as deltaic deposition, 500 m or 40% of the thickness of the sediments in the north that accumulated during the time of the Nyasa sequence cannot be accounted for by this mechanism; the maximum relief of a sedimentary structure in this kind of sedimentary environment is controlled by the depth of the lake, which again can be estimated in the order of 700 m. iii) During the deposition of the Boabab sequence, new fault segments were being formed, giving rise to the sub-basins south of the central sub-basin (Flannery and Rosendahl, 1990). iv) The fault scarp adjacent to the central segment is steep and looks morphologically fresh, indicating that this fault segment has been active during the Pleistocene.

Fig. 6 shows how these three faults increased their lengths and acquired displacement as each of the sequences were deposited. The overall evolutionary pattern is one in which, after an initial stage where the three fault segments grew with a symmetric slip distribution, the north and south segments then develop

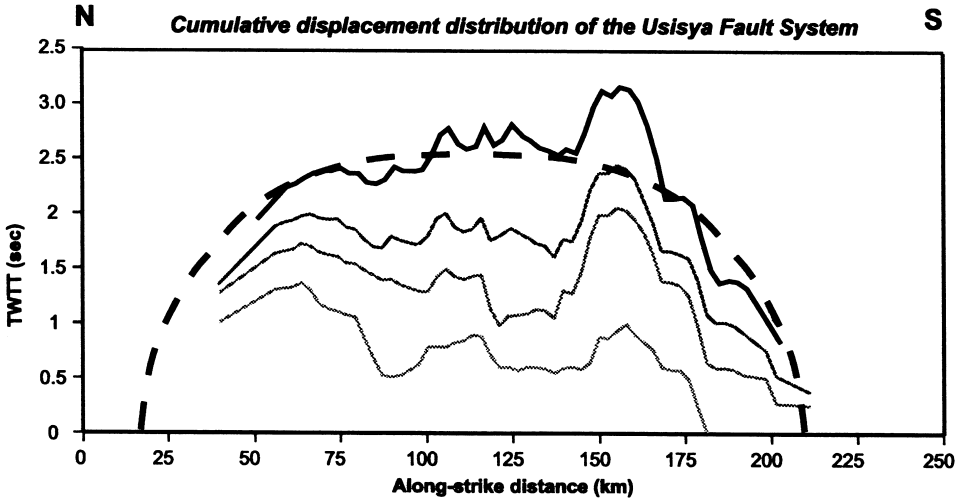

Fig. 7. Cumulative displacement profile of the Usisya fault system. This plot was obtained by adding the total displacement profiles in Fig. 5. It depicts how the fault system grew and acquired displacement through time. Vertical scale is two-way-travel-time in seconds.

asymmetric displacement profiles skewed preferentially toward the north and south, respectively, while the central fault segment maintained a symmetric displacement profile. Another feature of the central segment is that it accrued displacement without substantially increasing its length during the deposition of the Boabab and Mbamba sequences. Some of these features (asymmetry and steep displacement gradients in the relay ramp zone) have been observed in other populations of faults at smaller scales as well as in numerical experiments (Pollard and Segall, 1980; Willemse et al., 1996; Crider and Pollard, 1998).

The final total or summed displacement plot (Fig. 7) shows that the central segment had a displacement deficit during the early stages of rifting and that this deficit has almost been completely recovered by the time the Mbamba sequence was deposited (2.3–1.6 Ma), so that the summed displacement profile is consistent with the profile of other smaller normal faults (see Peacock and Sanderson, 1991; Dawers et al., 1993) and other large normal fault profiles (see Anders and Schlische, 1994; Cartwright et al., 1995; Schlische and Anders, 1996; Cartwright and Mansfield, 1998). Furthermore the estimated ratio of maximum displacement vs. the total length of the fault system is close to the ratios reported by these authors for individual isolated faults. The estimated length of the Usisya fault system is 170 km and has a maximum displacement of 6.4 km (including the water) on its south segment (Fig. 7) giving a ratio of 0.03. However individual fault segments do not follow this rule, and their ratios changed through time. The central fault evolved from a value of 0.042–0.053 (water corrected) during the deposition of the Nyasa sequence to a present value of 0.056–0.064; in a similar way, the south fault segment had an initial ratio of 0.07–0.092 that changed to a present ratio of 0.06–0.068. A feature of the developing total displacement profiles is the progression from three individual displacement maxima to just one within the respective intervals studied. During the intermediate interval, the summed displacement profile of the Boabab sequence displacement (Fig. 5b) shows two clear maxima developed in the region of overlap of the three segments. During deposition of the final sequence (Fig. 5c), the displacement profile shows a single displacement maxima. This pattern is obviously due to the shifting of activity from the northern and southern segments to the central one during deposition of the latest interval. However, the cumulative displacement profile (Fig. 7) shows a displacement deficit relative to a smoothed profile even for the final summing of displacement. The unanswered question is: as the fault continues to grow, would the final summed displacement exhibit a smoothed profile with the displacement maximum in the center?

5. Discussion and conclusions

An important observation first made by Peacock and Sanderson (1991) and observed in other studies of normal faults (Dawers and Anders, 1995; Cartwright et al., 1995; Willemse et al., 1996) is that segments that overlap one another exhibit steepened displacement gradients in the region of overlap. This results in a markedly larger displacement vs. length ratio than that of non-overlapping faults within the same tectonic environment (Dawers and Anders, 1995). Moreover, when two or more faults do finally physically link together, their combined length is significantly increased with respect to their maximum displacement. Dawers and Anders (1995) and Anders and Schlische

(1994) have suggested that there must be a rapid increase in displacement to account for the observed scaling relationship between displacement and length of linked faults. Peacock and Sanderson (1991) suggested that by summing the displacement for two overlapping faults, the final profile of displacement is achieved such that the maximum displacement becomes the region of overlap. Moreover, Simpson and Anders (1992) and Dawers and Anders (1995) have suggested that this strain accumulation is relieved in the overlap area by displacement being not only accrued on the main segments, but also on smaller overlapping faults. These interpretations of fault growth patterns imply that there is a time-dependence to the displacement in the region of overlap that previously has only been postulated. Moreover, if three segments link together, the final displacement must become a maximum in the central segment if scaling relationships are to be maintained in a fault system. Dawers and Anders (1995) suggested that during the growth process of a complex normal fault system involving three or more faults, the central segment would grow preferentially, eventually accruing the greatest displacement. Moreover, they suggested that the central segment did not necessarily have the greatest displacement rate prior to linkage, but that it grew faster after linkage. All these hypotheses were based on a final displacement pattern with no evidence of the surmised growth history. Here we have presented the first evidence that the growth pattern suggested by Peacock and Sanderson (1991), Anders and Schlische (1994), Dawers and Anders (1995) has indeed occurred as predicted. Furthermore, the temporal patterns observed on the Usisya fault system suggest that the generalized prediction of Nicol et al. (1997), that faults within a tectonic region that have accrued the greatest displacement always had higher displacement rates, is not generally applicable.

Gupta et al. (1998) have suggested that the evolution of a fault population has two distinctive stages: an initial stage characterized by the growth of faults nucleated independently with weak elastic interactions, followed by a stage of fault linkage where large faults grow by engulfing splays or adjacent smaller fault segments. Whether the faults of the Usisya fault system grew in this way remains an open question. However, the observations we have made are consistent with this generalized model of fault growth. One of the crucial areas in determining whether models such as these are appropriate is in the character of the displacement profile near the tip of the propagating faults. Unfortunately, our data give us the least information about the fault growth process in this region of fault overlap.

Anders and Schlische (1994) have suggested that regions of fault overlap correspond to intrabasin highs in the hanging wall basins. The Malawi basin is typical of many rift basins such as in the Basin and Range in that there is a clear pattern of intrabasin highs separating depocenters, which correspond to individual fault segment displacement maxima. Many neotectonic workers (e.g. Schwartz and Coppersmith, 1984) have implied that intrabasin highs are the locations of long-standing rupture barriers. The results of this study strongly support the idea that intrabasin highs are not necessarily regions of significant strain accumulation during the growth of a fault system. This is best seen in Fig. 5(b) where the displacements associated with the deposition of the Boabab sequence exhibit maximum displacement corresponding to the intrabasin highs (Fig. 5b). Clearly, regions of maximum total displacement are not the locations where faults are 'pinned' over long intervals. Anders and Schlische (1994) made this same point using patterns of footwall uplift which showed no consistent uplift deficit next to intrabasin highs for a large number of normal faults in the Basin and Range.

We conclude that the fault system evolved as follows.

1. About 8.6 Ma discrete depocenters started to form adjacent to the faults of the future bounding system. This probably corresponds to the isolated fault growth stage observed in numerical experimentation by Gupta et al. (1998). The northern segment was particularly active during this interval, and the highest displacement vs. length ratios were observed as fault overlap was just initiated.
2. During the deposition of the Boabab sequence, the southern segment became the most active. Also during this interval, all three main segments started to link together as evidenced by the higher displacement gradients toward the central segment, and by the cumulative displacement curve showing two maxima in the two regions of the overlap.
3. Between about 2.3 Ma and 1.6 Ma, the central segment was the most active. Tip gradients continued to increase, and although the central segment did not accrue sufficient displacement to exceed the total displacement of the two outer segments, the displacement to length ratio of the cumulative displacement on the fault system became 0.03, the value predicted for a single fault.

Initial linking together of individual segments increases the length relative to the fault system's cumulative displacements and the cumulative displacement vs. length ratio approached that of a single independent fault of length equal to the system length. Through gradual evolution of the fault system, the relationships between displacement and length progress toward a common value. It is our view that both the fault system, as well as segments within the system,

stabilize to a common displacement vs. length ratio that will be self-similar given enough time, as suggested by Dawers and Anders (1995).

Acknowledgements

The authors wish to thank Tom Blenkinsop and two anonymous reviewers for helpful comments. Support was provided by EAR 94-24487 (MHA), PRF 32194-AC2 (MHA), and EAR 97-06475 (CHS).

References

Anders, M.H., Spiegelman, M., Rodgers, D.W., Hagstrum, J.T., 1993. The growth of fault-bounded tilt blocks. Tectonics 12, 1451–1459.

Anders, M.H., Schlische, R.W., 1994. Overlapping faults, intrabasin highs, and the growth of normal faults. Journal of Geology 102, 165–180.

Cartwright, J.A., Trudgill, B.D., Mansfield, C.S., 1995. Fault growth by segment linkage; an explanation for scatter in maximum displacement and trace length data from the Canyonlands Grabens of SE Utah. Journal of Structural Geology 17, 1319–1326.

Cartwright, J.A., Mansfield, C.S., 1998. Lateral displacement variation and lateral tip geometry of normal faults in the Canyonlands National Park, Utah. Journal of Structural Geology 20, 3–19.

Crider, J.G., Pollard, D.D., 1998. Fault linkage: three-dimensional mechanical interaction between echelon normal faults. Journal of Geophysical Research 103, 24373–24391.

Dawers, N.H., Anders, M.H., Scholz, C.H., 1993. Growth of normal faults: Displacement–length scaling. Geology 21, 1107–1110.

Dawers, N.H., Anders, M.H., 1995. Displacement–length scaling and fault linkage. Journal of Structural Geology 17, 607–614.

Deng, J.S., Sykes, L.R., 1997. Evolution of the stress field in Southern California and triggering of moderate size earthquakes: a 200-years perspective. Journal of Geophysical Research 102, 9859–9886.

Ebinger, C.J., Denio, A.L., Tesha, A.L., Becker, T., Ring, U., 1993. Tectonic controls on rift basin morphology; evolution of the northern Malawi (Nyasa) rift. Journal of Geophysical Research 98, 17821–17836.

Flannery, J.W., Rosendahl, B.R., 1990. The seismic stratigraphy of Lake Malawi. Africa: Implications for interpreting geological processes in lacustrine rifts. Journal of African Earth Sciences 10, 519–548.

Gupta, S., Cowie, P.A., Dawers, N.H., Underhill, J.R.A., 1998. Mechanism to explain rift basin subsidence and stratigraphic patterns through fault array evolution. Geology 26, 595–598.

Hodgkinson, K.M., Stein, R.S., King, G.C.P., 1996. The 1954 Rainbow Mountain–Fairview Peak–Dixie Valley earthquakes: a triggered normal faulting sequence. Journal of Geophysical Research 101, 25459–25471.

King, G.C.P., Stein, R.S., Lin, J., 1994. Static stress changes and the triggering of earthquakes. Bulletin of the Seismological Society of America 84, 935–953.

Nicol, A., Walsh, J.J., Watterson, J., Underhill, J.R., 1997. Displacement rates of normal faults. Nature 390, 157–159.

Peacock, D.C.P., Sanderson, J., 1991. Displacement, segment linkage and relay ramps in normal fault zones. Journal of Structural Geology 13, 721–733.

Peacock, D.C.P., Sanderson, J., 1994. Geometry and development of relay ramps in normal faults systems. American Association of Petroleum Geologists Bulletin 78, 147–165.

Pollard, D.D., Segall, P., 1980. Mechanics of discontinuous faults. Journal of Geophysical Research 85, 4337–4350.

Rosendahl, B.R., 1987. Architecture of continental rifts with special reference to east Africa. Annual Revues in Earth and Planetary Science 15, 247–276.

Schlische, R.W., Young, S.S., Ackermann, R.V., Gupta, A., 1996. Geometry and scaling relations of a population of very small rift-related normal faults. Geology 24, 683–686.

Schlische, R.W., Anders, M.H., 1996. Stratigraphic effects and tectonic implications of the growth of normal faults and extensional basins. Geological Society of America Special Paper 303, 183–203.

Scholz, C.A. (Ed.), 1989. Project PROBE Geophysical Atlas Series, vol. 2. Duke University, Durham, North Carolina.

Scholz, C.A., 1997. Dynamic controls of rift-lake stratigraphy: lessons learned from seismic reflection imaging in the East African and Baikal rifts. Geological Society of America Abstracts with Programs 29, 6.

Schwartz, D.P., Coppersmith, K.J., 1984. Fault behavior and characteristic earthquakes; examples from the Wasatch and San Andreas fault zones. Journal of Geophysical Research 89, 5681–5698.

Simpson, D.W., Anders, M.H., 1992. Tectonic and topography of the Western United States: an application of digital mapping. GSA Today 2, 117–118; 120–121.

Spyropoulos, C., Scholz, C.H., Shaw, B.E., 1997. A model for the growth of a population of cracks. EOS, Transactions of the American Geophysical Union 78, 733.

Trudgill, B., Cartwright, J., 1994. Relay-ramp forms and normal-fault linkages. Canyonlands National Park, Utah. Geological Society of America Bulletin 106, 1143–1157.

Vening Meinesz, F.A., 1950. Les graben africans resultant de compression ou de tension dans le croute terrestre? Inst. R. Colon. Belge Bull 21, 539–552.

Willemse, E.J.M., Pollard, D.D., Aydin, A., 1996. Three-dimensional analyses of slip distributions on normal faults arrays with consequences for fault scaling. Journal of Structural Geology 18, 295–309.

Willemse, E.J.M., 1997. Segmented faults: correspondence between three-dimensional mechanical models and field data. Journal of Geophysical Research 102, 675–692.